

Homology Modeling of Cannabinoid Receptors: Discovery of Cannabinoid Analogues for Therapeutic Use

Chia-en A. Chang, Rizi Ai, Michael Gutierrez,
and Michael J. Marsella

Abstract

Cannabinoids represent a promising class of compounds for developing novel therapeutic agents. Since the isolation and identification of the major psychoactive component Δ^9 -THC in *Cannabis sativa* in the 1960s, numerous analogues of the classical plant cannabinoids have been synthesized and tested for their biological activity. These compounds primarily target the cannabinoid receptors 1 (CB1) and Cannabinoid receptors 2 (CB2). This chapter focuses on CB1. Despite the lack of crystal structures for CB1, protein-based homology modeling approaches and molecular docking methods can be used in the design and discovery of cannabinoid analogues. Efficient synthetic approaches for therapeutically interesting cannabinoid analogues have been developed to further facilitate the drug discovery process.

Key words: GPCR, Binding, Energy calculation, Molecular dynamics, Agonist

1. Introduction

The history of *Cannabis sativa* as a therapeutic agent has been well documented since 2737 BC (1) to its spread to India from China (2) and to its inclusion into the US Dispensatory in 1854 (3). The isolation of Δ^1 -tetrahydrocannabinol (Δ^9 -THC, also known as Δ^1 -THC) from *C. sativa* in 1964 (4) has since sparked much synthetic study and, more recently, intense pharmacological examination. As one of more than 60 cannabinoids found in cannabis, (-)- Δ^9 -THC (see Fig. 1) is responsible for the famous psychoactivity of cannabis and its therapeutic effects. The discovery of the cannabinoid receptors CB1 and CB2 and Δ^9 -THC analogues that selectively bind to those receptors have necessitated computer-aided drug design and a flexible synthetic pathway with high yields and stereoselectivity (5, 6).

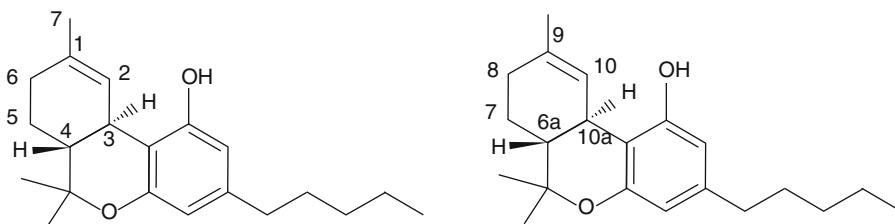
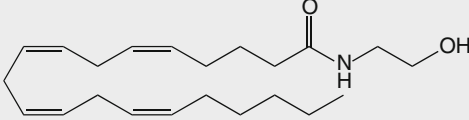
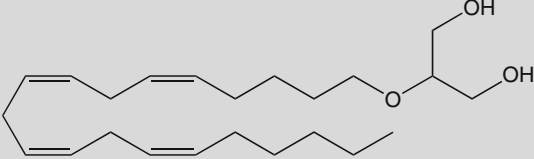
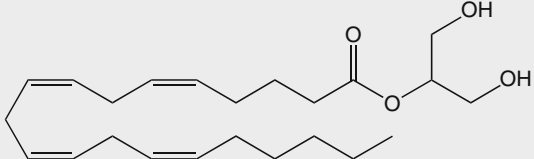
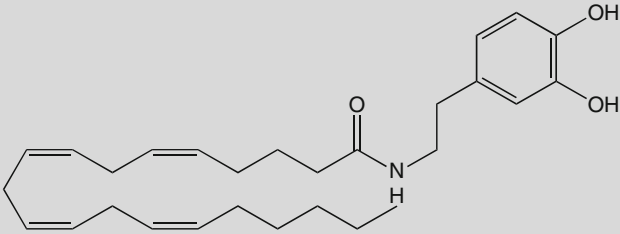



Fig. 1. Structure and numbering system of $(-)\text{-}\Delta^1\text{-THC}$ and $(-)\text{-}\Delta^9\text{-THC}$. *Left*: structure represents the monoterpene numbering; *Right*: structure represents the formal numbering.

Cannabinoids can be grouped into three classes: endogenous or endocannabinoids (naturally occurring cannabinoids found in the body), classical or natural (found in the plant species *Cannabis*), and nonclassical or synthetic (see Table 1). Endogenous cannabinoids, also known as eicosanoids, include anandamide, 2-arachidonoyl glycerol ether, 2-arachidonoyl glycerol (2-AG), *N*-arachidonoyl-dopamine (NADA), and virodhamine. The natural cannabinoids are similar in structure but do not all share the same bioactivity. These compounds have no significant psychotropic effects compared to $\Delta^9\text{-THC}$, however, they may have an impact on the effects of $\Delta^9\text{-THC}$ (7). Synthetic cannabinoids include dronabinol (Marinol), levonantradol, nabilone, and HU-210. It should be noted that some synthetic cannabinoids do not adhere to the typical structures found in the natural cannabinoids. More recently, intense pharmacological examinations have been carried out. For example, nabilone (Cesamet, Veleant Pharmaceuticals, Aliso Viejo, CA, USA) has been developed to suppress vomiting and nausea caused by chemotherapy and Marinol (Solvay Pharmaceuticals, Brussels, Belgium) for stimulating appetite in AIDS patients. Cannabinoids have therapeutic potential in a number of pathologic conditions, including mood and anxiety disorders, obesity and metabolic syndrome, movement disorders, neuropathic pain, spinal cord injury, and multiple sclerosis (8). Rimobabant, an antagonist of CB1, has been introduced to the market to treat obesity. Although the side effects of rimobabant severely limit the use of rimobabant and other CB1 antagonists, the therapeutically potential of drugs targeting CBs is still very high (9–11). CB1 drugs also have therapeutic potential in cancer, stroke, atherosclerosis, myocardial infarction, glaucoma, and osteoporosis (8).

Cannabinoids primarily target the CB1 and CB2 receptors but can interact with other proteins (12–14), and recent studies show that cannabinoid analogues target new receptor families (15, 16). CB1 receptor belongs to Class A (rhodopsin family) G-protein coupled receptors (GPCRs), but no experimental structures are available. A powerful tool for cannabinoid analogue design is use of structure-based approaches that require modeled

Table 1
Cannabinoid classes and structures

Name	Structure
Class: endocannabinoid	
Anandamide	
2-Arachidonoyl glycerol ether	
2-Arachidonoyl glycerol	
N-arachidonoyl-dopamine	
Virodhamine	

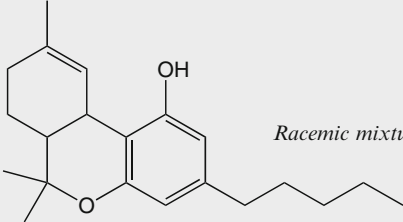
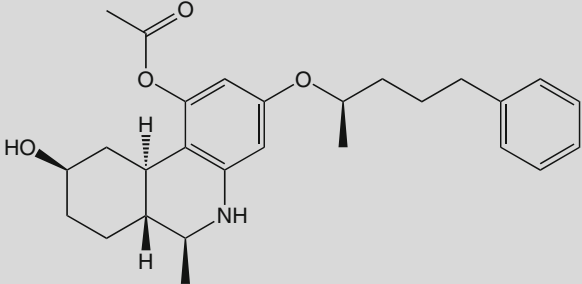
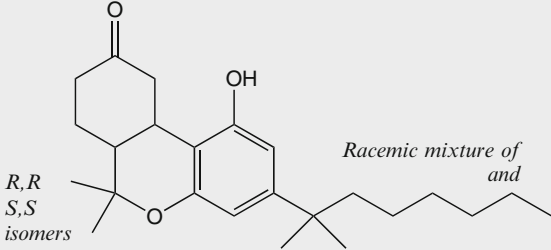
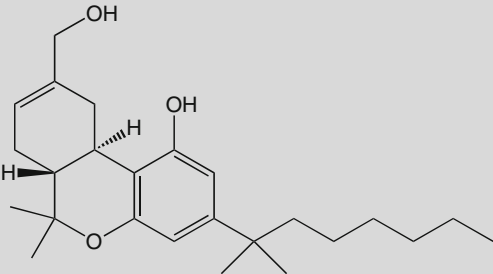
(continued)

Table 1
(continued)

Name	Structure
Class: classical/natural	
Delta-6 tetrahydrocannabinol	
Cannabinol	
Cannabicyclol	
Cannabigerol	
Cannabichromene	

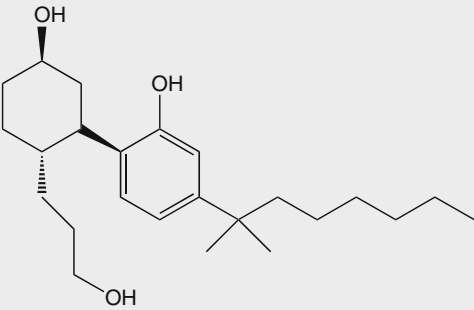
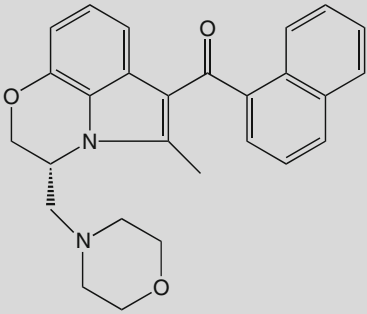
(continued)

Table 1
(continued)

Name	Structure
Class: nonclassical/synthetic	
Dronabinol (marinol)	 <p data-bbox="901 513 1130 581"><i>Racemic mixture of (±)-Δ^1-THC</i></p>
Levonantradol	
Nabilone	 <p data-bbox="602 1238 673 1306"><i>R,R</i> <i>S,S</i> <i>isomers</i></p> <p data-bbox="942 1209 1130 1257"><i>Racemic mixture of and</i></p>
HU-210	

(continued)

Table 1
(continued)

Name	Structure
CP-55,940	 <p>The chemical structure of CP-55,940 consists of a cyclohexane ring substituted with a hydroxyl group (OH) at the top position, a 3-(4-hydroxyphenyl)butyl group at the right position, and a 3-(3-hydroxypropyl) group at the bottom position. The 3-(4-hydroxyphenyl)butyl group is further substituted with a tert-butyl group and a pentyl chain.</p>
WIN-55,212-2	 <p>The chemical structure of WIN-55,212-2 features a central benzimidazole ring system. It is substituted with a morpholine ring at the 2-position, a methyl group at the 4-position, and a 1-(2-phenylphenyl)ethanone group at the 5-position.</p>

protein structures to predict the bound conformation and affinity of CB1 ligands. Up to late 2007, the structure of bovine rhodopsin (17–19) was the only high-resolution structure of GPCRs available as a template for homology modeling of CB1. Recently, a growing number of GPCR crystal structures have been reported and can be used for building new homology models; examples are the structures for human β_2 adrenergic receptor, turkey β_1 adrenergic receptor, human adenosine A_{2A} receptor, obvin opsin, and cxcR4 chemokine receptor (18, 20–25).

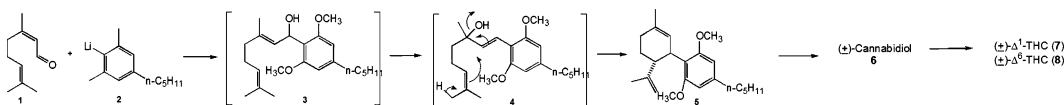
GPCRs exist in a conformational equilibrium between active and inactive states, but how the active and inactive states differ from each other is not exactly known. The binding of agonists to a GPCR may shift the equilibrium toward the active state, but some agonists may prefer binding to the receptor in its active state. Natural cannabinoids vary in their affinity and activity for the CB receptors, and Δ^9 -THC is known as a receptor agonist. Whether Δ^9 -THC binds

only to the active state of CB1 or whether can shift the protein from an inactive to active state is unknown. However, having a model structure that is in an active form or moving toward an active form is generally preferred in agonist drug discovery. Although most GPCR crystal structures used as templates for CB1 homology modeling are inactive, some structures encompass the structural features that have often been attributed to active GPCR conformations (26, 27). Therefore, after refinement and validation with known agonists, the CB1 models obtained from inactive GPCR templates may be considered active or toward-active structures.

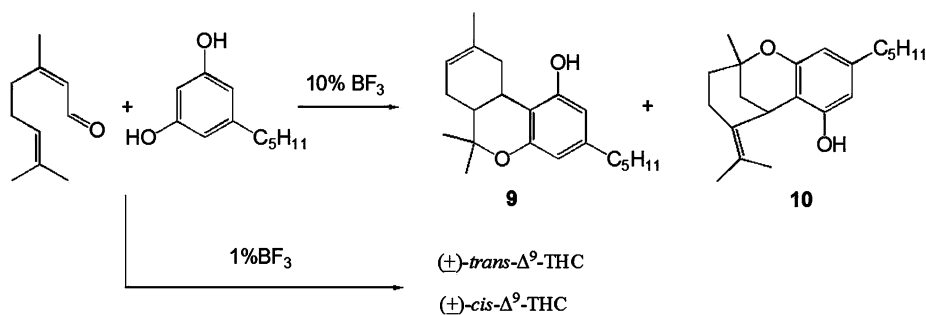
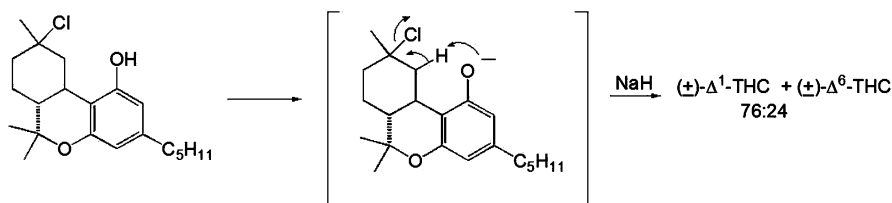
State-of-the-art molecular docking methods are useful for discovering new hits or leading optimization for computer-aided CB1 drug discovery and CB1 model refinement. Molecular docking of chemical libraries involves two steps: (1) the docking process aims accurately prediction of the pose of a compound within the protein binding site *in silico*; and (2) the scoring stage aims to score docked ligand–protein complexes by some measure to accurately predict the experimental binding affinity of the ligand to the target. Because more than one homology model is available from modeling and refinement processes, protein flexibility and docking may be incorporated. A chemical library can be docked into the protein to identify new binders and assist in modification of new compounds to be synthesized.

The first successful attempt at the synthesis of Δ^1 -THC was first reported by Gaoni and Mechoulam a year after they isolated the compound from plant material (4). Patterned after the proposed biogenetic pathway (28), citral was utilized (as opposed to geraniol) with the lithium derivative of olivetol dimethyl ether to afford a mixture thought to contain **3**. (\pm)-Dimethyl cannabidiol **5** was obtained after tosylation through a proposed allylic rearrangement **4**. **5** was demethylated at high temperatures with methylmagnesium iodide resulting in (\pm)-cannabidiol (**6**) and was subsequently converted to a mixture of (\pm)- Δ^9 -THC (**7**) and (\pm)- Δ^8 -THC (**8**) by acid treatment (see Scheme 1). The overall yield for the synthesis was only 2%.

Taylor et al. shortly thereafter reported a one-step synthesis (29) using citral and olivetol in 10% BF_3 to give (\pm)- Δ^8 -THC (**9**) in 10–20% yield and another compound later to be identified as an isocannabinoid (**10**) (28). By using hydrochloric acid in ethanol, Taylor was able to obtain the previously unsynthesized (\pm)-*cis*- Δ^9 -THC in 20% yield along with a small amount of the trans isomer, however was unable to separate the two isomers. Mechoulam and



Scheme 1. Mechoulam synthesis of (\pm)- Δ^1 -THC.

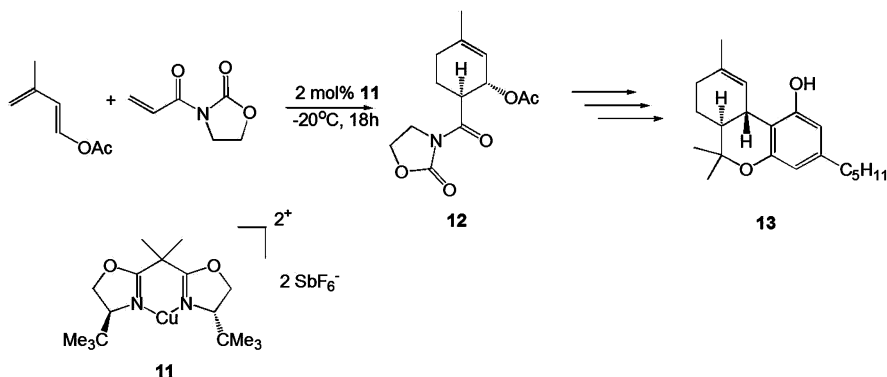
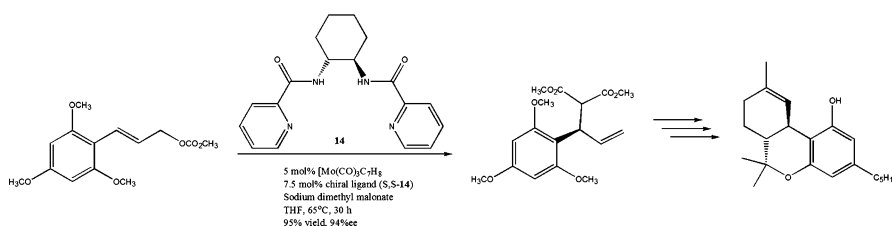
Scheme 2. Taylor synthesis and Mechoulam modification toward (\pm) - Δ^1 -THC and isomers.Scheme 3. Final step of Fahrenholtz synthesis of (\pm) - Δ^1 -THC.

coworkers were able to later modify Taylor's synthesis by using 1% BF_3 in methylene chloride to give (\pm) -*trans*- Δ^9 -THC in a 20% yield along with (\pm) -*cis*- Δ^9 -THC.¹² Scheme 2 summarizes these reactions.

In 1967, Fahrenholtz and coworkers reported an original synthesis of racemic Δ^9 -THC and Δ^8 -THC (and subsequently four of its isomers) in nine steps (30). Of particular interest was the final step in which the regioselectivity of this reaction is due to the formation of the phenolate ion and subsequent internal dehydrohalogenation, resulting in a 76:24 mixture of Δ^9 -THC: Δ^8 -THC (see Scheme 3).

In 1997, Evans et al. reported the first asymmetric synthesis of *S,S*- Δ^9 -THC using a bis(oxazoline)Cu(II) complex catalyzed Diels-Alder reaction as the key step for the asymmetric induction (31). Inspired by previous synthetic routes involving the use of monoterpenes that function as a hypothetical dictation synthon, the Evans group sought to create a chiral cycloadduct **12** from achiral starting materials to serve as their dictation synthon. Total synthesis of *S,S*- Δ^9 -THC (**13**) was accomplished in five steps with an overall yield of 21% (see Scheme 4).

While the Evans' synthesis was the first example of a stereospecific route to a THC isomer, synthesis of the actual stereoisomer found in cannabis (*R,R*- Δ^9 -THC) was not reported until 2007 by Trost and Dogra (32). Trost's retrosynthetic analysis includes setting all of the stereochemistry from a single Mo-catalyzed asymmetric allylic alkylation reaction. Use of this reaction and subsequent transformations toward *R,R*- Δ^9 -THC occurred in 17 steps with a 31% overall yield (see Scheme 5).

Scheme 4. Evans synthesis of *S,S*- Δ^9 -THC.Scheme 5. Trost-Synthesis of *R,R*- Δ^9 -THC.

2. Materials

2.1. Computer Skills and Programs

A typical desktop or laptop computer with 512 MB RAM and 500 MB free hard disk space is required. All web-based programs run on computers with Microsoft Windows and Apple Mac OS. A few modeling programs for fine-tuning CB1 models may need Linux or Unix operating systems.

The first step of homology modeling methods begins with the selection of suitable structural template(s) from the Protein Data Bank (PDB; <http://www.pdb.org>). Web servers such as SWISS-MODEL (<http://swissmodel.expasy.org/>) provide user-friendly interface to search for templates (33–35). The server also provides a template library, SWISS-MODEL template Library (ExPDB), which is derived from the PDB. A wide variety of alignment tools and homology modeling packages and servers such as T-coffee (<http://tcoffee.vital-it.ch/cgi-bin/Tcoffee/tcoffee.cgi/index.cgi>), MODELLER, Sybyl, Prime, and ICM, can be used to develop a homology model based on the selected template(s) (36). The results of alignment between our CB1 and the searched templates could be visualized with the DeepView program (<http://www.expasy.org/spdbv/>) (37). Accurate prediction of

the loops remains one of the most difficult aspects in the homology modeling. Software such as Prime may be used for loop optimization. Molecular dynamics (MD) simulations may be needed to fine-tune the modeled structures, especially for side-chain and loop conformations. Several molecular simulation packages such as Amber, Charmm, and Gromacs, provide energy minimization and MD methods to optimize protein conformation or ligand–protein interactions (38–40). A popular molecular graphics program VMD, which has a user-friendly interface to run an MD program NAMD, can be used for simple molecular modeling (41, 42).

2.2. Chemicals

Materials include a traditional synthetic chemistry workbench: a fume hood, balance, glassware, magnetic stirring apparatus, cooling bath, nitrogen gas, and chromatographic apparatus as described by Still et al. (43). Chemicals to prepare an authentic sample of (–)-*trans*- Δ^1 -THC include olivitol, (+)-*cis/trans*-*p*-mentha-2,8-dien-1-ol, anhydrous magnesium sulfate, BF₃ etherate, sodium bicarbonate, methylene chloride, Florisil, ethyl ether, and petroleum ether. All requisite environmental health and safety requirements must be met throughout the synthesis and including disposal of waste. It should be noted that natural cannabinoids are collectively classified as DEA Schedule I drugs.

3. Methods

3.1. Building Homology Models of CB1

The following procedures involved use of the SWISS-MODEL server to build CB1 models and can be broken down into the following steps:

1. Identification and selection of structural template(s).
2. Target sequence and template structure(s) alignment.
3. Model construction.
4. Model quality evaluation.

These steps can be repeated until a satisfying CB1 model is built.

3.1.1. Identification and Selection of Structural Template(s)

Experimentally determined structures of GPCRs are used as templates. The basic local alignment search tool (BLAST, <http://blast.ncbi.nlm.nih.gov/Blast.cgi>) is used for sequence similarity search. Before running the BLAST search, the human CB1 protein sequence (FASTA format) should be available. Here we used the human CB1 (brain) sequence downloaded from the NCBI protein database at: <http://www.ncbi.nlm.nih.gov/protein>.

```

3KJ6_A      DGRTGHLGRRSSKFCLKEHKALKTLGIIMGTFFTLCWLPFFIVNIVHVI-QDNLIRKEVYI
CB1         QVTRPDQARMDIRL-----AKTLVLILVLLIICWGPELLAIMVYDVFGKM

1F88_A      -----ATTQKAEKEVTRMVIIMVIAFLICWLPYAGVAFYIFTH-QGSDF
1U19_A      -----ATTQKAEKEVTRMVIIMVIAFLICWLPYAGVAFYIFTH-QGSDF
2R4R_A      -----GLRRSS-KFCLKEHKALKTLGIIMGTFFTLCWLPFFIVNIVHVIQ-DNLIR
2RH1_A      AKRVITTFRTGTWDAY-KFCLKEHKALKTLGIIMGTFFTLCWLPFFIVNIVHVIQ-DNLIR
3EML_A      AKRVITTFRTGTWDAYRSTLQKEVHAAKSLAIVGLFALCWLPPLHIINCFTFFC-PDCSH
3KJ6_A      -----GLRRSS-KFCLKEHKALKTLGIIMGTFFTLCWLPFFIVNIVHVIQ-DNLIR
CB1         -----RPDQARMDIRLAKTLVLILVLLIICWGPELLAIMVYDVFGKMNKLI

```

Fig. 2. Sequence alignment of CB1. *Top*: Alignment with PDB template code 3KJ6; *bottom*: multiple sequence alignment.

Templates that are close homologues of CB1 can usually be identified from a gapped BLAST query against the ExPDB template library extracted from the PDB (44). However, if no suitable template is identified or the sequence identity is too low, then two additional approaches can be used: the iterative profile blast, whereby the template library is searched with use of PSI-BLAST using an iteratively generated sequence profile, and the HHSearch, whereby the CB1 sequence is searched against a template library based on a hidden Markov model (44, 45).

Proteins with the best scores and/or sequence identities are selected as templates. Here we selected one human β_2 adrenergic receptor (pdb code: 3KJ6; 26% sequence identity with the CB1 sequence) and human adenosine A_{2A} receptor (pdb code: 3EML; 25% sequence identity with the CB1 sequence).

3.1.2. Target Sequence and Template Structure(s) Alignment

A critical step in constructing a good homology model is the initial alignment between the CB1 sequence and the template structure (s). Methods such as T-Coffee (<http://www.ebi.ac.uk/Tools/t-coffee/>), ClustalW (<http://www.ebi.ac.uk/Tools/clustalw2/>), MultAlign (<http://multalin.toulouse.inra.fr/multalin/>), and SALIGN (implemented in the MODELLER package) can be used for sequence alignment of membrane proteins (46–48). Because properly aligning CB1 may be difficult with use of a single template for sequence alignment, we used several similar GPCR sequences found by BLAST search for multiple sequence alignment of CB1 to generate a more accurate sequence alignment and thus a better model (see Note 1). The primary focus of multiple sequence alignment is to identify transmembrane regions that are highly conserved within several related sequences. Therefore, we used six protein sequences for multiple sequence alignment. (PDB codes for 3KJ6, human β_2 adrenergic receptor; 3EML, human adenosine A_{2A} receptor; 2RH1, human β_2 adrenergic receptor; 2R4R, human β_2 adrenergic receptor; and 1F88, bovine rhodopsin; 1U19, bovine rhodopsin.) An example is shown in Fig. 2. From CB1 domain assignment, the CB1 sequence RPDQARMDIRLAKTLVLILVLLIICWGPELLAIMVYDVF

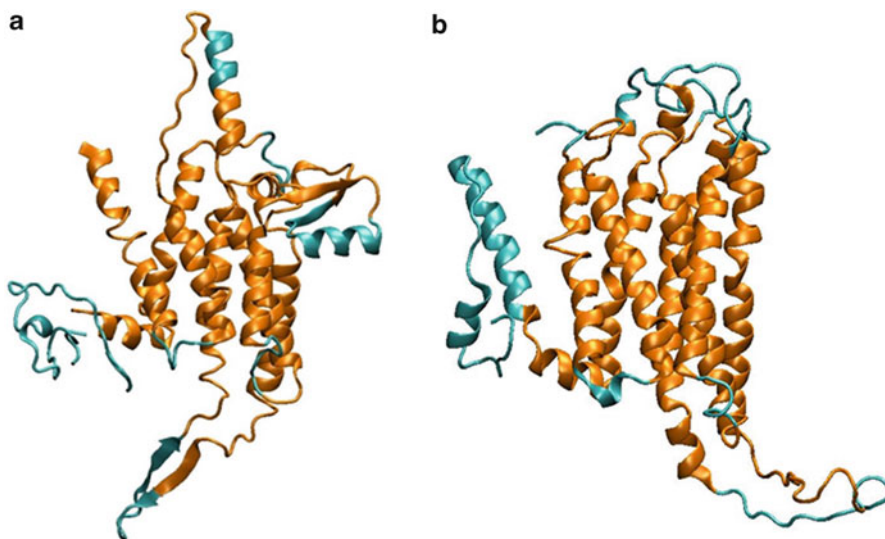


Fig. 3. Homology models of CB1. (a) A homology model built on the basis of PDB template 3KJ6; (b) a homology model built on the basis of the PDB template 3EML.

should be helix 6. If only one template, PDB 3KJ6, is used, the helix 6 is separated into two parts, but the use of more GPCRs sequences successfully avoids this problem.

3.1.3. Model Construction

Results of multiple sequence alignment are submitted in a CLUSTALW format to the SWISS-MODEL Alignment Mode, and users must provide a PDB code. The server pipeline builds a model based on the alignment result and an email is sent when the results are available. Two models based on different templates are shown in Fig. 3.

Figure 3 shows that use of different templates may result in very different structures. Figure 3b illustrates more reasonable transmembrane domains, but the structure in Fig. 3a does not have well-defined helices. To improve the model, one can build seven transmembrane helices individually and then assemble each fragment (see Note 2). The server provides methods for predicting secondary structures which are useful for constructing the CB1 models; examples are InterProdomain Scan, PsiPred for secondary structure prediction and DISOPRED for disorder prediction. Figure 4 shows the helix 2 from two models that are not yet good models, with the final helix structure based on predicting the length of the helix, as well as further alignment with only helix 2 and not including the whole protein. Regions that cannot be modeled well with standard homology modeling can also be used with the protein threading methods to build the structure. Servers are available for the protein threading, e.g., WURST: <http://www.zbh.uni-hamburg.de/wurst/> (49).

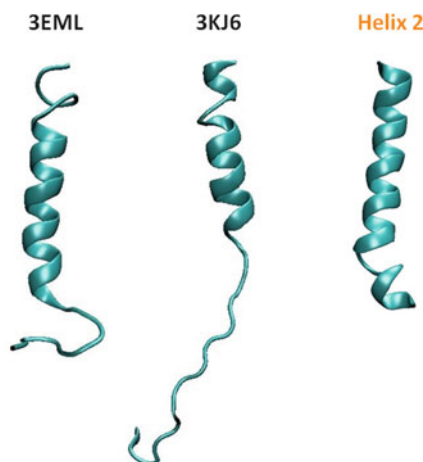


Fig. 4. Modeled structures of helix 2 based on PDB codes 3EML and 3KJ6, and the final helix structure based on predicted helix 2 region.

In most cases, side-chain and loop conformations need to be modeled in a further step after the backbone is constructed. SCWRL is a widely used program for adding side-chains to a protein backbone based on a backbone-dependent rotamer library (50). The program has a library that provides lists of chi1-chi2 pairs for residues at given phi-psi values, and explores these pairs to try to minimize possible conformation clashes. Other programs, such as OPUS-Rota, apply similar ideas for adding side-chains (51).

3.1.4. Model Quality Evaluation

Evaluation of the quality of the final model(s) is a crucial step in homology modeling and can be assessed using Ramachandran maps and with programs such as Procheck, Whatcheck, and QMEAN implemented in the SWISS-MODEL web server (52–54). The model can be further validated by docking a known binder into the binding site and checking whether the model contains protein–ligand contact suggested by experiments. For example, experimental mutation studies suggested that residue Lys3.28 forms important interactions with Δ^9 -THC. If such interactions are missing, then the model should be further refined as described in the following section.

3.2. Modification, Refinement, and Validation of CB1 Models

Because evidence shows that all GPCRs share a common fold, the seven transmembrane helices are relatively easier to model by using standard protocol in the SWISS-MODEL server or the MODELLER program. Moreover, a recent study of 105 ns MD simulations of the CB1 receptor embedded in a lipid bilayer revealed that the helical bundle structures of the CB1 receptor retain a structure similar to the overall X-ray structure of GPCRs (55). However, long loops and side-chains may need further

refinement, especially for the residues near the ligand binding site (see Note 3). To obtain a more accurate structure, one can embed a homology model in a pre-equilibrium lipid bilayer combined with a water box to model and refine the protein in a more realistic environment. Standard minimization and equilibrium procedures can be carried out and the entire system can be sampled by MD simulations. Although programs such as GROMACS and NAMD provide tools for membrane protein modeling, some technical details depend on systems (40, 41). Moreover, because the system is huge, the MD simulations need to be run in a large cluster.

A solution to avoid high demand of computer time and time-consuming setup, one can focus on residues near the binding site by relaxing the atoms near the binding site and fixing most parts of the transmembrane helical domains during the MD simulations. To optimize CB1 side-chain and backbone conformations for a known binder, a compound such as Δ^9 -THC may be docked into the binding site and then the MD simulations can be carried out for the ligand-protein complex. The VMD program provides an NAMD graphic interface with which users can easily fix atoms, add water, and run energy minimization and MD simulations. To avoid unrealistic in vacuo Coulombic interactions, if a ligand is not present in the binding site, programs can be used to add a water box near the binding site or a desired number of waters can be added manually into the binding site. Standard simulation procedures such as assigning parameters to the protein and ligands can be found in NAMD, VMD, and AMBER manuals (<http://www.ks.uiuc.edu/Research/vmd/>, <http://www.ks.uiuc.edu/Research/namd/> and <http://ambermd.org/doc11/Amber11.pdf>).

3.3. Structure-Based Drug Screening: Docking and Scoring Methods

Once the CB1 models are validated, docking methods can be used in drug discovery for finding lead compounds, lead optimization, and scaffold hopping. A wide variety of docking methods are in use for virtual screening, and some, such as DOCK and AUTODOCK, are free of charge for academic researchers (56, 57). CB1 presumably has a large binding pocket and is reasonably flexible, because structurally very different ligands, such as endocannabinoid and natural cannabinoids, can bind tightly in the binding site. Although some programs may allow protein side-chains to move during the docking process, the backbone is held fixed. As a result, if CB1 adapts to a significantly different conformation upon ligand binding, the docking program cannot capture it.

In considering protein flexibility, more than one CB1 structures, especially different models refined by different classes of ligands or structures with different backbone conformations, can be considered for docking. After each docked pose is available, a scoring function ranks the best energy pose of each ligand. Evaluating docked compounds by different scoring functions has received much attention recently (58). Top-scoring compounds

are usually subjected to ad hoc evaluation, such as formation of specific van der Waals contacts and ligand–receptor hydrogen bonds. This extra stage also helps compensate for intrinsic deficiencies in the scoring function and in knowledge-based ligand design.

In the absence of experimental 3D structures of the ligand-CB1 complex, known binders are docked into CB1 models to predict the ligand–receptor complex structure, gain a better understanding of the ligand binding determinants, guide compound modification, lead optimization, and develop virtual combinatorial libraries. Chemical databases such as the National Cancer Institute (NCI) and ZINC database, can also be used for virtual screening to identify new leads or scaffolds. Instead of screening thousands of compounds, an NCI diversity set of about 1,500 compounds representing the broader chemical space of the 140,000 in the full NCI database may be docked for the initial screen. 3D structures of the ligands should be prepared before docking them into CB1. The 3D structures of ligands may be available in web pages such as PubChem <http://pubchem.ncbi.nlm.nih.gov/> and sd or mol files can be downloaded. The Olson Laboratory also distributes the NCI diversity set formatted for use in AutoDock (59). If 3D structures are not available, 2D structures can be drawn with tools such as ChemDraw and converted to 3D structures. Of note, a 2D to 3D converter may not result in reasonable energy minima of ligands which are needed for docking, particularly ligands with flexible ring conformations (see Note 4). As a result, conformational search methods such as Vconf can be used to generate an optimized ring conformation (60).

3.4. Synthetic Tools for Cannabinoid Analogues

The synthesis of authentic (–)-*trans*- Δ^1 -THC can be prepared most easily using the method of Razdan (61). A round-bottom flask is charged with a magnetic stir bar, methylene chloride (as solvent, adjusted to 0.1M w/r to olivitol), 1 equivalent of olivitol, 1 equivalent of (+)-*cis/trans-p*-mentha-2,8-dien-1-ol, and 2 equivalents anhydrous magnesium sulfate. The solution is stirred using a magnetic stirplate, cooled using an ice-water bath, and kept air-free via manipulating under nitrogen gas environment. BF_3 etherate is added (1% based on the volume of methylene chloride) and the reaction allowed stirred for 1.5 h. The reaction is quenched with a solution of aqueous sodium bicarbonate and the resulting organic phase is isolated using a separatory funnel. The organic layer is dried over anhydrous magnesium sulfate, and volatiles removed under reduced pressure to afford a crude product as a viscous oil. Pure THC can be isolated by chromatography on Florisil using graded eluent mixtures ranging from pure petroleum ether to 2:98 ethyl ether : petroleum ether. The reported yield is ca. 30%.

4. Notes

1. The CBI sequence should have high similarity with a template sequence. If not, multiple templates need to be selected for multiple sequence alignment for better alignment results.
2. Because CBI is a huge protein, building a good homology model by considering the whole protein, including helices and loops together may be challenging. The target CBI sequence can be split into smaller fragments. For example, one or two transmembrane helices with a connecting loop can be considered as a fragment. Alignment and secondary structure determination can involve use of the sequences of each fragment to obtain a better model. Then, fragments can be assembled on the basis of the selected templates. Note that the helical bundles have similar topology, so the transmembrane domains are relatively easy to assemble. Other tools described in Subheading 2 might be needed for constructing extracellular domains.
3. A common problem is that flexible loop regions are missing in crystal structures. In addition, the extracellular regions may be less conserved between CBI and other GPCR templates. Protein threading, loop prediction, and MD simulations can be used to build the flexible parts.
4. Natural cannabinoids such as Δ^9 -THC, have ring structures with different stereoisomers. When preparing ligands for docking studies, attention must be paid to use a correct conformation of stereoisomer because docking programs change only the conformations of the rotatable bonds but not the ring conformations.

References

1. Li, H. L. 1974. Origin and Use of Cannabis in Eastern Asia Linguistic-Cultural Implications. *Economic Botany* 28:293–301.
2. Mechoulam, R. 1986. *Cannabinoids as Therapeutic Agents*. CRC Press.
3. Robson, P. 2001. Therapeutic aspects of cannabis and cannabinoids. *British Journal of Psychiatry* 178:107–115.
4. Gaoni, Y., and R. Mechoulam. 1964. ISOLATION STRUCTURE + PARTIAL SYNTHESIS OF ACTIVE CONSTITUENT OF HASHISH. *Journal of the American Chemical Society* 86:1646–8.
5. Matsuda, L. A., S. J. Lolait, M. J. Brownstein, A. C. Young, and T. I. Bonner. 1990. STRUCTURE OF A CANNABINOID RECEPTOR AND FUNCTIONAL EXPRESSION OF THE CLONED CDNA. *Nature* 346:561–564.
6. Munro, S., K. L. Thomas, and M. Abushaar. 1993. MOLECULAR CHARACTERIZATION OF A PERIPHERAL RECEPTOR FOR CANNABINOIDS. *Nature* 365:61–65.
7. Ashton, J. C., I. Appleton, C. L. Darlington, and P. F. Smith. 2004. Cannabinoid CBI receptor protein expression in the rat choroid plexus: a possible involvement of cannabinoids in the regulation of cerebrospinal fluid. *Neuroscience Letters* 364:40–42.
8. Pacher, P., S. Batkai, and G. Kunos. 2006. The endocannabinoid system as an emerging target of pharmacotherapy. *Pharmacological Reviews* 58:389–462.

9. Bellocchio, L., G. Mancini, V. Vicennati, R. Pasquali, and U. Pagotto. 2006. Cannabinoid receptors as therapeutic targets for obesity and metabolic diseases. *Current Opinion in Pharmacology* 6:586–591.
10. Steinberg, B. A., and C. P. Cannon. 2007. Cannabinoid-1 receptor blockade in cardiometabolic risk reduction: Safety, tolerability, and therapeutic potential. *American Journal of Cardiology* 100:27P–32P.
11. Kunos, G., and D. Osei-Hyiaman. 2008. Endocannabinoids and liver disease. IV. Endocannabinoid involvement in obesity and hepatic steatosis. *American Journal of Physiology-Gastrointestinal and Liver Physiology* 294:G1101–G1104.
12. Ross, R. A. 2007. Allosterism and cannabinoid CB1 receptors: the shape of things to come. *Trends in Pharmacological Sciences* 28:567–572.
13. Begg, M., P. Pacher, S. Batkai, D. Osei-Hyiaman, L. Offertaler, F. M. Mo, H. Liu, and G. Kunos. 2005. Evidence for novel cannabinoid receptors. *Pharmacology & Therapeutics* 106:133–145.
14. Harkany, T., M. Guzman, I. Galve-Roperh, P. Berghuis, L. A. Devi, and K. Mackie. 2007. The emerging functions of endocannabinoid signaling during CNS development. *Trends in Pharmacological Sciences* 28:83–92.
15. Pertwee, R. G. 2005. The therapeutic potential of drugs that target cannabinoid receptors or modulate the tissue levels or actions of endocannabinoids. *Aaps Journal* 7:E625–E654.
16. Howlett, A. C. 2002. The cannabinoid receptors. *Prostaglandins & Other Lipid Mediators* 68-9:619–631.
17. Palczewski, K., T. Kumasaka, T. Hori, C. A. Behnke, H. Motoshima, B. A. Fox, I. Le Trong, D. C. Teller, T. Okada, R. E. Stenkamp, M. Yamamoto, and M. Miyano. 2000. Crystal structure of rhodopsin: A G protein-coupled receptor. *Science* 289:739–745.
18. Park, J. H., P. Scheerer, K. P. Hofmann, H. W. Choe, and O. P. Ernst. 2008. Crystal structure of the ligand-free G-protein-coupled receptor opsin. *Nature* 454:183–U133.
19. Murakami, M., and T. Kouyama. 2008. Crystal structure of squid rhodopsin. *Nature* 453:363–U333.
20. Wacker, D., G. Fenalti, M. A. Brown, V. Katritch, R. Abagyan, V. Cherezov, and R. C. Stevens. 2010. Conserved Binding Mode of Human beta(2) Adrenergic Receptor Inverse Agonists and Antagonist Revealed by X-ray Crystallography.
21. Bokoch, M. P., Y. Z. Zou, S. G. F. Rasmussen, C. W. Liu, R. Nygaard, D. M. Rosenbaum, J. J. Fung, H. J. Choi, F. S. Thian, T. S. Kobilka, J. D. Puglisi, W. I. Weis, L. Pardo, R. S. Prosser, L. Mueller, and B. K. Kobilka. 2010. Ligand-specific regulation of the extracellular surface of a G-protein-coupled receptor.
22. Jaakola, V. P., M. T. Griffith, M. A. Hanson, V. Cherezov, E. Y. T. Chien, J. R. Lane, A. P. Ijzerman, and R. C. Stevens. 2008. The 2.6 Angstrom Crystal Structure of a Human A (2A) Adenosine Receptor Bound to an Antagonist. *Science* 322:1211–1217.
23. Warne, T., M. J. Serrano-Vega, J. G. Baker, R. Moukhametzianov, P. C. Edwards, R. Henderson, A. G. W. Leslie, C. G. Tate, and G. F. X. Schertler. 2008. Structure of a beta(1)-adrenergic G-protein-coupled receptor.
24. Scheerer, P., J. H. Park, P. W. Hildebrand, Y. J. Kim, N. Krauss, H. W. Choe, K. P. Hofmann, and O. P. Ernst. 2008. Crystal structure of opsin in its G-protein-interacting conformation.
25. Wu, B., E. Y. Chien, C. D. Mol, G. Fenalti, W. Liu, V. Katritch, R. Abagyan, A. Brooun, P. Wells, F. C. Bi, D. J. Hamel, P. Kuhn, T. M. Handel, V. Cherezov, and R. C. Stevens. 2010. Structures of the CXCR4 chemokine GPCR with small-molecule and cyclic peptide antagonists.
26. Mobarec, J. C., R. Sanchez, and M. Filizola. 2009. Modern Homology Modeling of G-Protein Coupled Receptors: Which Structural Template to Use? *Journal of Medicinal Chemistry* 52:5207–5216.
27. Schwartz, T. W., and W. L. Hubbell. 2008. Structural biology - A moving story of receptors. *Nature* 455:473–474.
28. Mechoulam, R. 1973. Marijuana. *Chemistry Metabolism, Pharmacology and Clinical Effects*. Academic Press, New York.
29. Taylor, E. C., K. Lenard, and Y. Shvo. 1966. ACTIVE CONSTITUENTS OF HASHISH. SYNTHESIS OF DL-DELTA6-3,4-TRANS-TETRAHYDROCANNABINOL. *Journal of the American Chemical Society* 88:367-&.
30. Mechoula, R., P. Braun, and Y. Gaoni. 1972. SYNTHESSES OF DELTA-TETRAHYDROCANNABINOL AND RELATED CANNABINOIDS. *Journal of the American Chemical Society* 94:6159-&.
31. Evans, D. A., E. A. Shaughnessy, and D. M. Barnes. 1997. Cationic bis(oxazoline)Cu(II) Lewis acid catalysts. Application to the asymmetric synthesis of ent-Delta(1)-tetrahydrocannabinol. *Tetrahedron Letters* 38:3193–3194.

32. Trost, B. M., and K. Dogra. 2007. Synthesis of (-)-Delta(9)-trans-Tetrahydrocannabinol: Stereocontrol via Mo-catalyzed asymmetric allylic alkylation reaction. *Organic Letters* 9:861–863.
33. Arnold, K., L. Bordoli, J. Kopp, and T. Schwede. 2006. The SWISS-MODEL workspace: a web-based environment for protein structure homology modelling.
34. Kiefer, F., K. Arnold, M. Kunzli, L. Bordoli, and T. Schwede. 2009. The SWISS-MODEL Repository and associated resources.
35. Peitsch, M. C. 1995. Protein Modeling by E-Mail (Vol 13, Pg 658, 1995).
36. N. Eswar, M. A. M.-R., B. Webb, M. S. Madhusudhan, D. Eramian, M. Shen, U. Pieper, A. Sali. 2006. Comparative Protein Structure Modeling With MODELLER. John Wiley & Sons, Inc.
37. Guex, N., and M. C. Peitsch. 1997. SWISS-MODEL and the Swiss-PdbViewer: An environment for comparative protein modeling.
38. Case, D. A., T. E. Cheatham, T. Darden, H. Gohlke, R. Luo, K. M. Merz, A. Onufriev, C. Simmerling, B. Wang, and R. J. Woods. 2005. The Amber biomolecular simulation programs.
39. Brooks, B. R., C. L. Brooks, A. D. Mackerell, L. Nilsson, R. J. Petrella, B. Roux, Y. Won, G. Archontis, C. Bartels, S. Boresch, A. Caffisch, L. Caves, Q. Cui, A. R. Dinner, M. Feig, S. Fischer, J. Gao, M. Hodoscek, W. Im, K. Kuczera, T. Lazaridis, J. Ma, V. Ovchinnikov, E. Paci, R. W. Pastor, C. B. Post, J. Z. Pu, M. Schaefer, B. Tidor, R. M. Venable, H. L. Woodcock, X. Wu, W. Yang, D. M. York, and M. Karplus. 2009. CHARMM: The Biomolecular Simulation Program.
40. Van der Spoel, D., E. Lindahl, B. Hess, G. Groenhof, A. E. Mark, and H. J. C. Berendsen. 2005. GROMACS: Fast, flexible, and free.
41. Phillips, J. C., R. Braun, W. Wang, J. Gumbart, E. Tajkhorshid, E. Villa, C. Chipot, R. D. Skeel, L. Kale, and K. Schulten. 2005. Scalable molecular dynamics with NAMD. *Journal of Computational Chemistry* 26:1781–1802.
42. Humphrey, W., A. Dalke, and K. Schulten. 1996. VMD: Visual molecular dynamics. *Journal of Molecular Graphics* 14:33–&.
43. Still, W. C., M. Kahn, and A. Mitra. 1978. RAPID CHROMATOGRAPHIC TECHNIQUE FOR PREPARATIVE SEPARATIONS WITH MODERATE RESOLUTION. *Journal of Organic Chemistry* 43:2923–2925.
44. Altschul, S. F., T. L. Madden, A. A. Schaffer, J. H. Zhang, Z. Zhang, W. Miller, and D. J. Lipman. 1997. Gapped BLAST and PSI-BLAST: a new generation of protein database search programs.
45. Soding, J. 2005. Protein homology detection by HMM-HMM comparison (vol 21, pg 951, 2005).
46. Forrest, L. R., C. L. Tang, and B. Honig. 2006. On the accuracy of homology modeling and sequence alignment methods applied to membrane proteins. *Biophysical Journal* 91:508–517.
47. Notredame, C., D. G. Higgins, and J. Heringa. 2000. T-Coffee: A novel method for fast and accurate multiple sequence alignment. *Journal of Molecular Biology* 302:205–217.
48. Thompson, J. D., D. G. Higgins, and T. J. Gibson. 1994. CLUSTAL-W - IMPROVING THE SENSITIVITY OF PROGRESSIVE MULTIPLE SEQUENCE ALIGNMENT THROUGH SEQUENCE WEIGHTING, POSITION-SPECIFIC GAP PENALTIES AND WEIGHT MATRIX CHOICE. *Nucleic Acids Research* 22:4673–4680.
49. Torda, A. E., J. B. Procter, and T. Huber. 2004. Wurst: a protein threading server with a structural scoring function, sequence profiles and optimized substitution matrices.
50. Krivov, G. G., M. V. Shapovalov, and R. L. Dunbrack. 2009. Improved prediction of protein side-chain conformations with SCWRL4.
51. Lu, M. Y., A. D. Dousis, and J. P. Ma. 2008. OPUS-Rota: A fast and accurate method for side-chain modeling. *Protein Science* 17:1576–1585.
52. Laskowski, R. A., M. W. Macarthur, D. S. Moss, and J. M. Thornton. 1993. Procheck - a Program to Check the Stereochemical Quality of Protein Structures.
53. Hoof, R. W. W., G. Vriend, C. Sander, and E. E. Abola. 1996. Errors in protein structures.
54. Benkert, P., S. C. E. Tosatto, and D. Schomburg. 2008. QMEAN: A comprehensive scoring function for model quality assessment.
55. Shim, J. Y. 2009. Transmembrane Helical Domain of the Cannabinoid CB1 Receptor. *Biophysical Journal* 96:3251–3262.
56. Lang, P. T., S. R. Brozell, S. Mukherjee, E. F. Pettersen, E. C. Meng, V. Thomas, R. C. Rizzo, D. A. Case, T. L. James, and I. D. Kuntz. 2009. DOCK 6: Combining techniques to model RNA-small molecule complexes. *Rna-a Publication of the Rna Society* 15:1219–1230.
57. Osterberg, F., G. M. Morris, M. F. Sanner, A. J. Olson, and D. S. Goodsell. 2002. Automated docking to multiple target structures: Incorporation of protein mobility and structural water heterogeneity in AutoDock.

- Proteins-Structure Function and Bioinformatics 46:34–40.
58. Feher, M. 2006. Consensus scoring for protein-ligand interactions. *Drug Discovery Today* 11:421–428.
 59. Morris, G. M., D. S. Goodsell, R. S. Halliday, R. Huey, W. E. Hart, R. K. Belew, and A. J. Olson. 1998. Automated docking using a Lamarckian genetic algorithm and an empirical binding free energy function. *Journal of Computational Chemistry* 19:1639–1662.
 60. Chang, C. E., and M. K. Gilson. 2003. Tork: Conformational analysis method for molecules and complexes. *Journal of Computational Chemistry* 24:1987–1998.
 61. Razdan, R. K., H. C. Dalzell, and G. R. Handrick. 1974. HASHISH.10. SIMPLE ONE-STEP SYNTHESIS OF (-)-TETRAHYDROCANNABINOL (THC) FROM PARAMENTHA-2,8-DIEN-1-OL AND OLIVETOL. *Journal of the American Chemical Society* 96:5860–5865.